Triangular Ising antiferromagnet in a staggered field

Abhishek Dhar
Condensed Matter Theory Unit, Jawaharlal Nehru Centre for Advanced Scientific Research, Bangalore 560064, India

Pinaki Chaudhuri and Chandan Dasgupta*
Department of Physics, Indian Institute of Science, Bangalore 560012, India

(Received 25 August 1999)

We study the equilibrium properties of the nearest-neighbor Ising antiferromagnet on a triangular lattice in the presence of a staggered field conjugate to one of the degenerate ground states. Using a mapping of the ground states of the model without the staggered field to dimer coverings on the dual lattice, we classify the ground states into sectors specified by the number of ''strings.'' We show that the effect of the staggered field is to generate long-range interactions between strings. In the limiting case of the antiferromagnetic coupling constant J becoming infinitely large, we prove the existence of a phase transition in this system and obtain a finite lower bound for the transition temperature. For finite J, we study the equilibrium properties of the system using Monte Carlo simulations with three different dynamics. We find that in all the three cases, equilibration times for low-field values increase rapidly with system size at low temperatures. Due to this difficulty in equilibrating sufficiently large systems at low temperatures, our finite-size scaling analysis of the numerical results does not permit a definite conclusion about the existence of a phase transition for finite values of J. A surprising feature in the system is the fact that unlike usual glassy systems, a zero-temperature quench almost always leads to the ground state, while a slow cooling does not.

I. INTRODUCTION

The triangular Ising antiferromagnet (TIAFM), described by the Hamiltonian

$$H = J\sum_{\langle i,j\rangle} s_i s_j \quad J>0, \tag{1}$$

where $s_i = \pm 1$ and $\langle i,j\rangle$ denotes nearest-neighbor sites on a triangular lattice, provides an interesting example of a frustrated system without disorder. Unlike the nearest-neighbor Ising antiferromagnet on a square lattice, this model does not have a finite-temperature phase transition. It has an exponentially large number of degenerate ground states, which implies that the zero-temperature entropy per spin is finite. The zero-field partition function can be computed exactly, leading to the result $S(T=0)=0.3383\ldots$ (Ref. 1) for the zero-temperature entropy per spin. At zero temperature, the system is critical and the two-spin correlation function decays as a power law, $c(r)\sim\cos(2\pi r/3)/r^{1/2}$, along the three principal directions.[2] The ground states of the TIAFM can be mapped exactly to dimer coverings on the dual lattice, which is hexagonal.[3] Using this mapping, it is possible to classify the ground states into sectors specified by the number of ''strings'' that represent the difference between two dimer coverings.

The exponential degeneracy of the ground state of the TIAFM can be removed in various ways, e.g., by choosing different coupling constants along the three principal directions, or by introducing a uniform field. Both these cases have been extensively studied. For anisotropic couplings, the problem is exactly solvable[4] and one finds a usual Ising-like second-order phase transition except in some special cases for which the transition temperature goes to zero. In the case of a uniform field, simulations and renormalization-group arguments[5] indicate that there is a second-order transition belonging to the three-state Potts model universality class.

A particularly interesting special case is the limit in which the system is restricted to remain within the manifold of the TIAFM ground states. This can be achieved by making the coupling constant J infinitely large. One then considers the effects of degeneracy breaking terms. In this limit, the nature of the transition changes. In the case of anisotropic couplings, the transition changes from Ising-like to Kastelyn-type (K-type).[6] Below T_c, the system freezes into the ground state and the specific heat vanishes identically. As T_c is approached from the high-temperature side, the specific heat shows a $(T-T_c)^{-1/2}$ singularity. In the case of a uniform applied field, the transition is believed to be of Kosterlitz-Thouless type.[7] This case is treated by first mapping the problem to a solid-on-solid model and then using renormalization-group arguments.

In this paper, we study the behavior of the TIAFM in the presence of a staggered field chosen to be conjugate to one of the ground states. Our work is motivated in part by similar studies on glassy systems[8] with exponentially large number of metastable states. These studies consider the thermodynamic behavior of such systems in the presence of a field conjugate to a typical configuration of an identical replica of the system. As the strength of the field is increased from zero, the system is found to undergo a first-order transition in which the overlap with the selected configuration changes discontinuously. This transition is driven by the competition between the energy associated with the field term and the configurational entropy arising from the presence of an exponentially large number of metastable states. Like these glassy systems, the TIAFM has frustration and an exponentially large number of ground states. Thus it is of interest to

investigate whether a similar behavior is present in the TIAFM, which is a simpler model with no externally imposed quenched disorder. Besides, the question of whether a phase transition can occur in the TIAFM in the presence of an ordering field is interesting by itself. For systems with a finite number of ground states, such as the purely ferromagnetic Ising model and the Ising antiferromagnet on a bipartite lattice, it can be proved that no phase transition can occur in the presence of ordering fields.[9] However, no such general proof exists for systems with an exponentially large number of ground states, and the question of whether a competition between the energy associated with the ordering field and the extensive ground-state entropy can drive a phase transition in such systems remains open.

The staggered field considered by us is conjugate to a ground state with alternate rows of up and down spins. In the lattice-gas picture of the Ising model, this corresponds to an applied potential that is periodic in the direction transverse to the rows. In the presence of the field, there are a large number of low-lying energy states and this suggests the possibility of an interesting phase transition as the temperature is varied. We consider the case where the coupling constant J is finite, as well as the limit $J\to\infty$. In the latter limit, one considers only the set of states that are ground states of the TIAFM Hamiltonian of Eq. (1). In this limit, we show that the problem of evaluating the partition function reduces to calculating the largest eigenvalue of a one-dimensional fermion Hamiltonian with long-range Coulombic interactions. We have not been able to solve this problem but have obtained a finite lower bound for the transition temperature. The transition appears to be K-type.

For finite J, we have studied the equilibrium behavior of the system by Monte Carlo (MC) simulations using three different kinds of dynamics: (1) single-spin-flip Metropolis dynamics, (2) cluster dynamics, and (3) ''string'' dynamics in which all the spins on a line are allowed to flip simultaneously. We find that in all three cases, equilibration times at low fields and low temperatures increase rapidly with system size. The last dynamics is found to be the most efficient one for equilibrating the system in this regime. Finite-size scaling analysis of the data for small fields suggests the existence of a characteristic temperature near which the correlation length becomes very large. However, because of the long equilibration times, we have not been able to study large enough systems to be able to answer conclusively the question of whether this corresponds to a true phase transition.

One surprising finding of our study concerns zero-temperature quenches of the system, starting from random initial configurations. We show that the system almost always reaches the ground state in such quenches. On the other hand, a slow cooling of the system leads to a metastable state. This is contrary to what happens in usual glassy systems where a fast quench usually leads to the system getting stuck in a higher-energy state, while a slow cooling leads to the ground state with a high probability.

The paper is organized as follows. In Sec. II, we consider the TIAFM in zero field and describe the mapping from the ground states to dimer coverings and the subsequent classification of the ground states into sectors. Many of the results in this section are well-known, but we have included them for the sake of completeness. Also our description is somewhat different from the existing ones. In Sec. III, we consider the TIAFM with an applied staggered field in the limit $J\to\infty$. The mapping of this system to a one-dimensional fermion model is described and a finite lower bound for the transition temperature is derived. In Sec. IV, we present our numerical results for the equilibrium properties at finite J. These results are obtained from exact numerical evaluation of averages using transfer matrices and also through MC simulations. We also discuss the dynamic behavior of the system under different MC procedures. Section V contains a summary of our main results and a few concluding remarks.

II. MAPPING OF TIAFM GROUND STATES TO DIMER COVERINGS AND CLASSIFICATION INTO STRING SECTORS

The frustration of the TIAFM arises from the fact that it is impossible to satisfy all three bonds of any elementary plaquette of the triangular lattice. At most we can have two bonds satisfied. The lowest-energy configuration of the system is one in which every elementary triangle is maximally satisfied. This condition can be satisfied for a large number of configurations and for future reference we shall denote the set of all such states by $\mathcal{G}$. We now show the correspondence between the ground states and dimer coverings on the dual lattice. The dual lattice is formed by taking the centers of all the triangles. Consider any two triangles that share a bond. If the bond is not satisfied, we place a dimer connecting the centers of the two triangles. The fact that every triangle has one and only one unsatisfied bond implies that every point of the dual lattice forms the end point of one and only one dimer. Hence we obtain a dimer covering. This mapping is not unique, since flipping all spins in any given spin configuration leads to the same dimer covering. In Fig. 1 we show a ground-state configuration and the corresponding dimer covering. Another dimer covering that corresponds to a ground state with alternate rows of up and down spins is shown in Fig. 2. We shall call this the standard configuration. It is important to choose the boundary conditions in a convenient manner and we follow the convention used in Fig. 1 with periodicity in the x and y directions.

A useful classification of the ground states is obtained by superposing the standard dimer configuration with any other dimer configuration. This results in string configurations as shown, for example, in Fig. 3, which is obtained by superposing the standard configuration of Fig. 2 with the configuration of Fig. 1. Clearly there is a one-to-one correspondence between string and dimer configurations.

It is easy to prove the following points: (i) the number of strings passing though every row is conserved; (ii) the strings do not intersect; (iii) the number of strings can be any even number from 0 to L, where L is the number of spins in a row; (iv) the periodic boundary conditions mean that the strings have to match at the boundaries and form closed loops.

We classify the ground states into different sectors, with each sector specified by the number of strings. The number of states in each sector can be counted exactly using transfer matrices. Let us label the bonds on successive rows of the lattice in the manner shown in Fig. 4. The position of the strings on each row is specified by the set of numbers $\{b_1, b_2, \ldots b_n\}$, where b_k gives the position of the kth

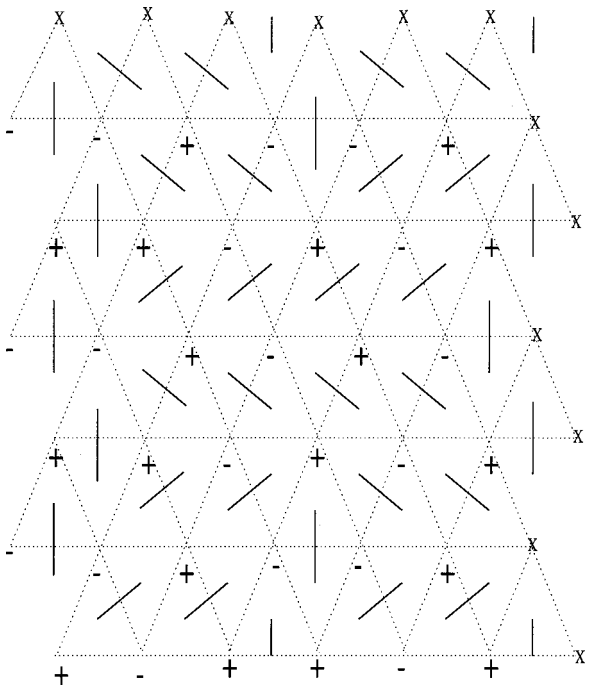

FIG. 1. A ground-state configuration and the corresponding dimer covering for a 6×6 lattice. Periodic boundary conditions are applied in the horizontal and vertical directions. The crosses correspond to repeated points.

string. Note that $\{b_k\}$ give the positions of the satisfied bonds in a row. In a sector with n strings we consider the ${}^{L}C_n\times{}^{L}C_n$ matrix, which has nonvanishing entries equal to one if the two states can be connected by string configurations. We need two different transfer matrices, namely $T^{(1)}$, which transfers from odd-numbered rows to even-numbered ones and $T^{(2)}$, which transfers from even to odd ones. The total number of states in any given sector is then given by

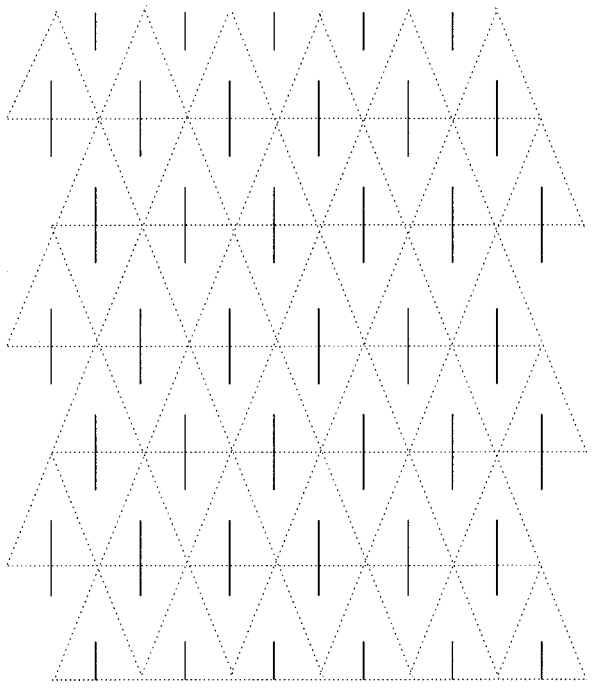

FIG. 2. The standard configuration of dimers.

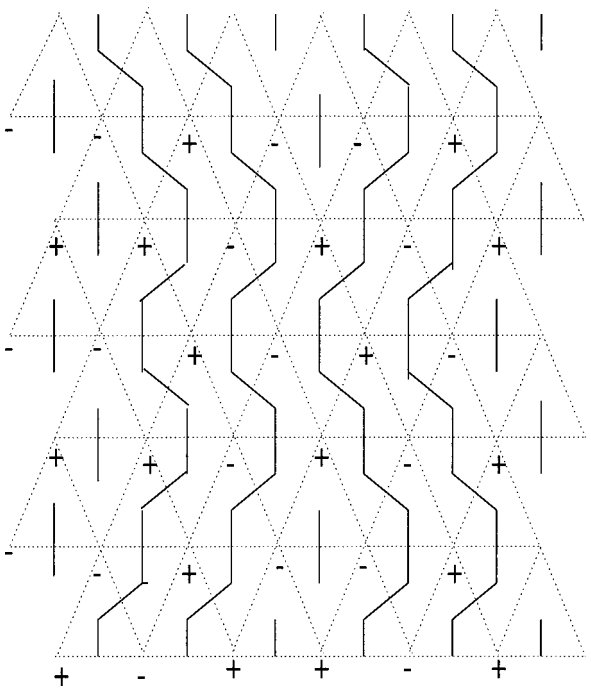

FIG. 3. A configuration of strings obtained by superposing the dimer configurations in Fig. 1 and Fig. 2.

$$\mathcal{N}(n)=Tr(T^{(1)}T^{(2)})^{L/2}, \tag{2}$$

where we choose, for convenience, the length of the lattice L to be even.

As an example let us consider the transfer matrix in the two-string sector. This is given by

$$T^{(1)}_{(l_1,l_2)|(l_3,l_4)}=\delta_{l_1,l_3}\delta_{l_2,l_4}+\delta_{l_1,l_3-1}\delta_{l_2,l_4}+\delta_{l_1,l_3}\delta_{l_2,l_4-1}$$
$$+\delta_{l_1,l_3-1}\delta_{l_2,l_4-1}\quad\text{for}\quad l_2\neq l_1+1,$$

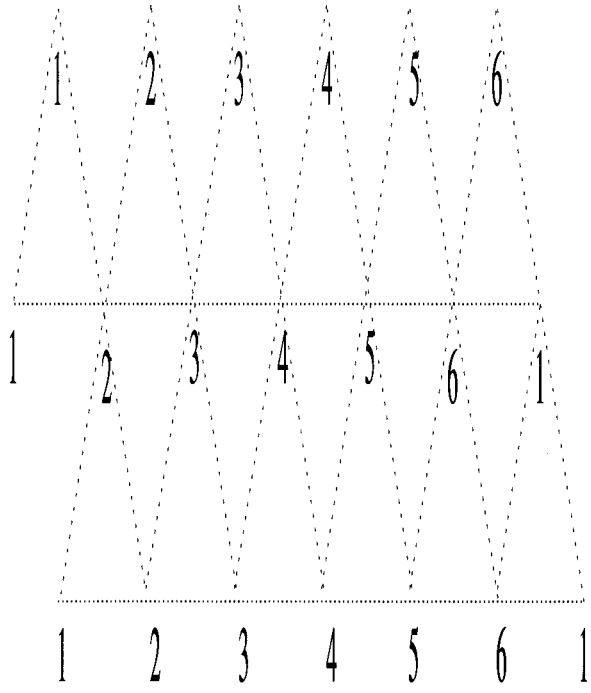

FIG. 4. Labeling of successive rows on a 6×6 lattice.

$$T^{(1)}_{(l_1,l_1+1)|(l_3,l_4)} = \delta_{l_1,l_3}\delta_{l_1+1,l_4} + \delta_{l_1,l_3}\delta_{l_1+1,l_4-1} + \delta_{l_1,l_3-1}\delta_{l_1+1,l_4-1}. \quad (3)$$

The matrix is diagonalized by the antisymmetrized plane-wave eigenstates

$$a_{l_1,l_2} = e^{i(q_1 l_1 + q_2 l_2)} - e^{i(q_1 l_2 + q_2 l_1)}, \quad q_1 < q_2. \quad (4)$$

The periodic boundary condition leads to the following values for the wave vectors: $q_i = (2n_i+1)\pi/L$, with $n_i = 0,1,2,\ldots L-1$. The eigenvalues are given by

$$\lambda^{(1)}_q = (1+e^{iq_1})(1+e^{iq_2}). \quad (5)$$

The matrix $T^{(2)}$ has the same set of eigenvectors, while the eigenvalues are given by

$$\lambda^{(2)}_q = (1+e^{-iq_1})(1+e^{-iq_2}). \quad (6)$$

The results for the two-string sector can be generalized to any of the other sectors. The transfer matrices $T^{(1)}$ and $T^{(2)}$ in any sector are diagonalized by antisymmetrized plane-wave states. This just reflects the fact that the strings can be thought of as the world lines of noninteracting fermions. The eigenvalues in the n-string sector are

$$\lambda^{(1)}_q = \prod_{k=1}^{n} (1+e^{iq_k}),$$

$$\lambda^{(2)}_q = \prod_{k=1}^{n} (1+e^{-iq_k}), \quad (7)$$

with q_ks as before. The number of states in the n-string sector is thus given by

$$\mathcal{N}(n) = Tr(T^{(1)}T^{(2)})^{L/2} = \sum_{q_1<q_2\ldots.q_n} \left[\prod_{k=1}^{n} (1+e^{iq_k})(1+e^{-iq_k})\right]^{L/2}. \quad (8)$$

In the large L limit, only the dominant term in the above sum contributes and we finally obtain

$$\mathcal{N}(p) = e^{L^2\alpha(p)},$$

$$\alpha(p) = p\ln 2 + \frac{2}{\pi}\int_0^{\pi p/2} dx \ln[\cos(x)], \quad (9)$$

where $p = n/L$ is the fraction of strings (''string density''). Thus every sector with nonzero p has an exponentially large number of states.

We note that the function $\alpha(p)$ is peaked at $p = 2/3$ and the entropy of this sector, $S = \alpha(2/3)$, reproduces the well-known result of Wannier for the zero-temperature entropy of the TIAFM. Thus we have rederived Wannier's result and also shown that most of the states are in the sector with string density equal to 2/3.

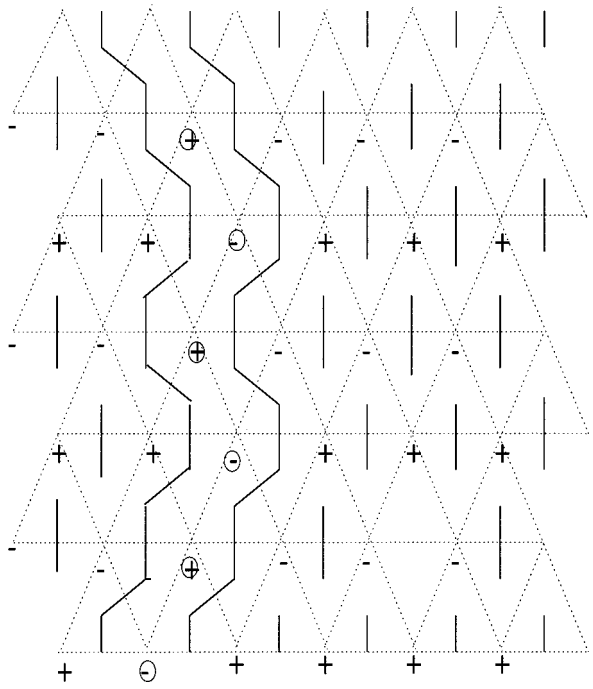

FIG. 5. A configuration of two strings that corresponds to the lowest-energy state in this sector. This configuration is obtained by starting with the ground state and flipping a line of spins (the circled ones). The strings are closely packed and all the spins in the region between them point opposite to the local applied fields.

III. SPLITTING OF LEVELS IN THE PRESENCE OF A STAGGERED FIELD: THE $J \to \infty$ LIMIT

In the presence of a staggered field h that is conjugate to one of the ground states of the TIAFM, the macroscopic degeneracy of the ground state is lifted. The field we consider is conjugate to the state corresponding to the standard dimer configuration (Fig. 2). There are two such spin configurations and we choose the one that has all up spins on the first row. Note that in the presence of the field, any two states related by the flipping of all the spins have the same string representation but different energies. To remove this ambiguity, we use an additional label for the string states, which we take as the sign of the first spin in the first row. The spin configuration on any row is then fully specified by the set $(s, b_1, b_2, \ldots b_n)$.

Let us now look at the effect of the field in splitting the energy levels in each sector. In the zero-string sector there are two states, one corresponding to the ground state and the other, obtained by flipping all spins, to the highest-energy state. The lowest-energy states in the two-string sector can be generated by starting with the ground-state spin configuration and flipping a line of spins as shown in Fig. 5. Figure 6 shows a higher-energy two-string state. Note that the strings separate the lattice into two domains, one in which all the spins point along the staggered-field directions and another in which they point opposite to the field. This is, in general, true for any n-string state where the strings divide the lattice into n domains, with spins in alternate domains pointing along and opposite to the staggered fields. The lowest-energy configuration in any sector is clearly the state with alternate pairs of strings tightly packed. For the sector in which the string density is p, the lowest energy per spin is

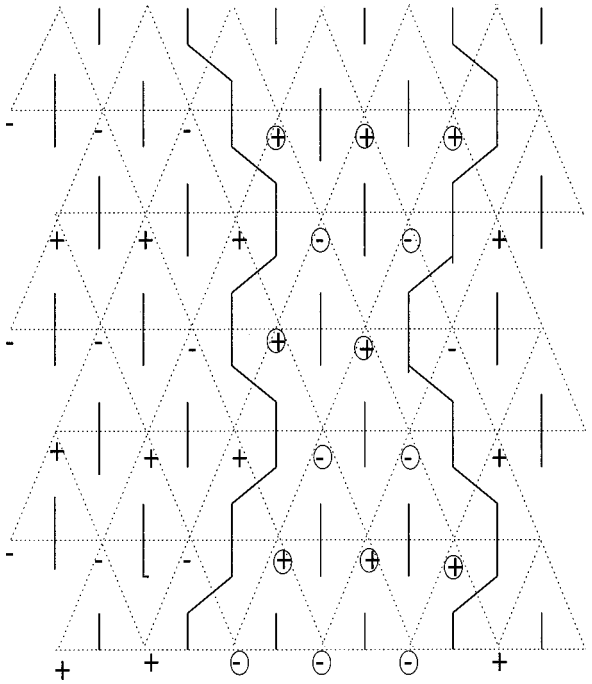

FIG. 6. A higher-energy configuration in the two-string sector. It can be seen that the strings divide the lattice into two domains with the spins in one domain being along the applied field and opposite to it (the circled spins) in the other domain.

$$e_g(p) = -(1-p)h, \tag{10}$$

where for the case $J \to \infty$ being considered here, we have subtracted the infinite constant energy term $-J$.

Because of the conservation of the number of strings across rows, the transfer matrix is block diagonal, each block corresponding to a fixed string sector. In the zero-field case the strings are noninteracting and the problem reduced essentially to that of free fermions on a line. In the present case, however, the energy increases when the separation between two strings is increased. In fact, it is easy to see that this case reduces to a one-dimensional fermion problem in which every alternate pair of fermions interact with each other via an attractive linear potential. It is then no longer simple to diagonalize the transfer matrix. However, through the following argument we prove the existence of a phase transition and obtain a lower bound for the transition temperature. At zero temperature, the system will be in the ground state in the zero-string sector. As the temperature is increased, the entropic factor associated with the other sectors becomes important and can cause either a gradual or a sharp transition to other sectors. To determine which of the two possibilities actually occurs, we consider the simpler case where the strings do not interact and all configurations belonging to the sector with string density p have the same energy $Ne_g(p)$, where $N = L^2$ is the total number of spins. Since all the states in this sector have energies greater than or equal to $Ne_g(p)$ in the interacting model, a sharp transition in the noninteracting case implies a sharp transition in the interacting model. In particular, if the noninteracting model exhibits a transition at temperature T_c, so that it is frozen in the ground state in the zero-string sector for $T \leqslant T_c$, then the interacting model must also be in the ground state for all $T \leqslant T_c$. In other words, the transition temperature of the noninteracting model provides a lower bound to the transition temperature of the interacting model.

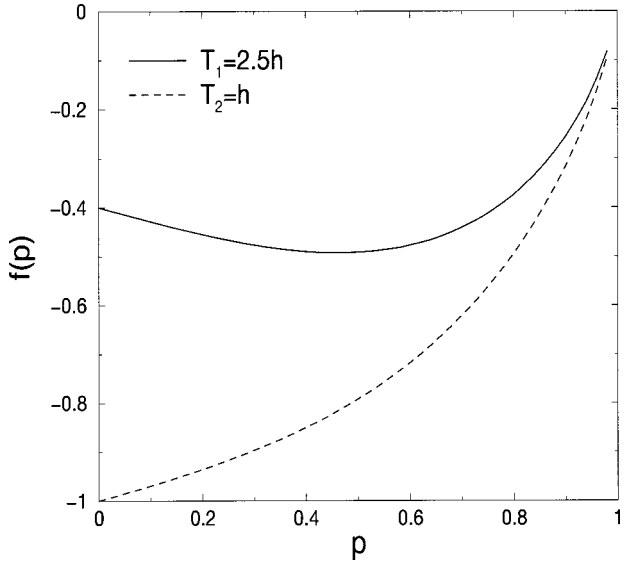

FIG. 7. The dimensionless free energy $f(p)$ of the noninteracting model, plotted as a function of the string density p at two different temperatures, $T_1 = 2.5h$, which is above T_c, and $T_2 = h$, which is below T_c.

The partition function of the noninteracting model may be written as

$$Z = \sum_p e^{N\alpha(p) - \beta N e_g(p)} = e^{N[\alpha(p_m) - \beta e_g(p_m)]}, \tag{11}$$

where $\beta = 1/T$ and p_m is the value of p corresponding to the minimum of the function $f(p) = -\alpha(p) + \beta e_g(p)$. Using Eq. (9) and Eq. (10), we get

$$p_m = 0, \quad T < T_c,$$
$$p_m = \frac{2}{\pi}\cos^{-1}\left(\frac{e^{h/T}}{2}\right), \quad T > T_c, \tag{12}$$

with $T_c = h/\ln(2)$. Thus, there exists a sharp transition at a finite temperature T_c, the number of strings being identically zero below this temperature. In Fig. 7, we show the dimensionless free-energy function $f(p)$ at two different temperatures, one above and one below T_c. It can be seen that for $T < T_c$, the function $f(p)$ has its lowest value at $p = 0$. The minimum of $f(p)$ moves continuously away from $p = 0$ as the temperature is increased above T_c, approaching $p = 2/3$ in the $T \to \infty$ limit.

In Fig. 8, we have plotted p_m, the equilibrium value of the string density obtained from Eq. (12), as a function of T/h. It is easy to see from Eq. (12) that p_m grows as $(T - T_c)^{1/2}$ as T is increased above T_c. Since the internal energy is proportional to p_m in the noninteracting model, the specific heat vanishes identically for $T < T_c$ and diverges as $(T - T_c)^{-1/2}$ for T approaching T_c from above. Thus we get a K-type transition that is expected because of the equivalence of our system to dimer models. While this proves the exis-

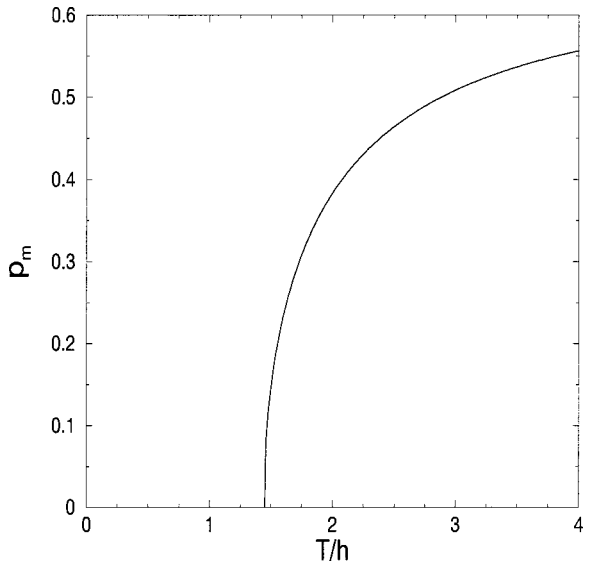

FIG. 8. The equilibrium string density p_m plotted as a function of the temperature T (measured in units of h) for the noninteracting string model.

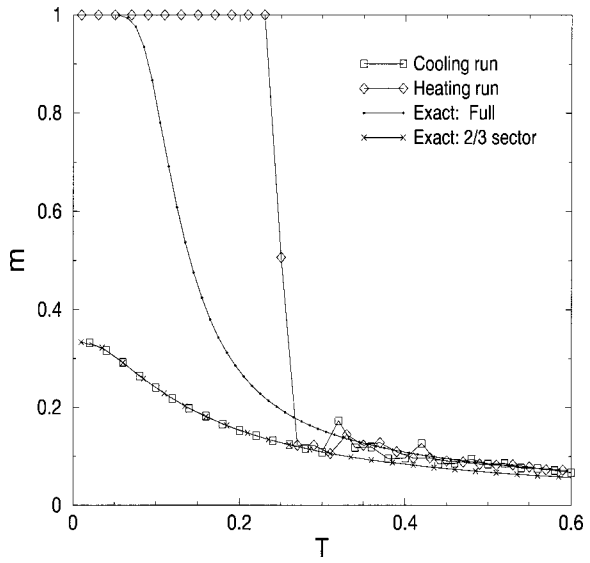

FIG. 9. Results for the staggered magnetization m, obtained from single-spin-flip MC heating and cooling runs for a 6×6 system with $h=0.05$ and $J=1$. Also shown are the results of exact numerical evaluation of the staggered magnetization for $J=1$, and the staggered magnetization in the $p=2/3$ sector for $J\to\infty$.

tence of a transition in the interacting model too, it is not clear whether the nature of the transition is the same.[15] It is quite possible that the long-range interactions between the strings would result in a transition in a different universality class. This issue is addressed in the next section.

It is interesting to compare our model with the model with anisotropic couplings studied by Blöte and Hilhorst.[6] Consider the case when the horizontal couplings have strength $(J-\Delta)$ and the remaining two are of strength J. In the limit $J\to\infty$, we need to consider only the states within $\mathcal{G}$. In this case too, the ground state lies in the zero-string sector but is twofold degenerate since the up-down symmetry is retained. The excitations are again in the form of strings but are noninteracting and so equivalent to the excitations in the simplified model considered by us. In fact the expression for the free energy in Eq. (11) follows directly from Eq. (2) in Ref. 6 if we make the identification $h=2\Delta$.

IV. MC SIMULATIONS AND TRANSFER-MATRIX CALCULATIONS FOR FINITE J

For finite J, we have carried out MC simulations to determine whether the phase transition persists and its nature if it does. A problem with the simulations is that equilibration times are very long for small values of h/J and T/J. We have tried to overcome this problem by performing simulations with three kinds of dynamics. However, even with the fastest dynamics, we have been able to obtain reliable data only for relatively small system sizes ($L\leqslant18$). We have also carried out exact numerical evaluations of averages using transfer matrices for small samples. The results obtained from these numerical calculations are described below.

A. Single-spin-flip Metropolis dynamics

In Fig. 9 we show the results of a MC simulation using the standard single-spin-flip Metropolis dynamics.[10] We have plotted the staggered magnetization m as a function of temperature T for a heating run and a cooling run on a 6×6 system. The staggered field and the coupling constant are set to $h=0.05$ and $J=1.0$, respectively (unless otherwise stated, all the numerical results reported in this section are for $J=1.0$). The data shown were obtained by averaging over 10^6 MC steps per spin (MCS). The heating run was started from the ground state in the zero-string sector and the cooling run started from a random spin configuration. It is clear from the data that even for this small system, equilibration is not obtained for temperatures lower than about 0.3. We also examined the states obtained by starting the system in a random configuration and then quenching it instantaneously to zero temperature. We find that the system then goes to the lowest-energy state in one of the many sectors. For example, in the simulation corresponding to Fig. 9, the system reached the zero-string ground state. On heating, the system continues to be in the zero-string sector until at some temperature value it jumps to the high-temperature phase. On the other hand, a slow cooling from the high-temperature phase leads to the lowest-energy state in the $p=(2/3)$ sector and the true zero-string ground state is not reached.

These results can be understood as follows. As discussed in the preceding section, the ground state lies in the zero-string sector, and the excitations within $\mathcal{G}$ from the ground state correspond to the formation of an even number of strings. The single-spin-flip dynamics is reasonably efficient in exploring the states within a sector with a fixed number of strings. However, at low temperatures, it is extremely ineffective in changing the number of strings. In fact, even with zero external field, the single-spin-flip dynamics at zero temperature is nonergodic and only samples states within a given sector. At finite temperatures, the only way to change the number of strings is through moves which take the system out of $\mathcal{G}$. These moves cost energy of order J. At low temperatures, the probability of acceptance of such moves becomes extremely small. Thus in Fig. 9, during the heating run, the system starts from the ground state in the zero-string sector and stays stuck in it till the temperature is sufficiently

high. At high temperatures, the $p=2/3$ sector is most probable (note that at very high temperatures, the string picture is no longer valid) and during the cooling run, the system starts from this sector and again stays stuck in this sector since the dynamics cannot reduce the number of strings. Thus the cooling curve basically shows equilibrium properties within the $p=2/3$ sector.

We have verified the above picture by an exact numerical evaluation of the staggered magnetization for a 6×6 system. This is done by numerically computing the two sums that occur in the expression

$$m=\frac{1}{N}\langle M\rangle=\frac{1}{N}\frac{Tr[M(V^{(1)}V^{(2)})^{L/2}]}{Tr[(V^{(1)}V^{(2)})^{L/2}]}, \tag{13}$$

where $V^{(1),(2)}$ are the usual row-to-row transfer matrices and M is a diagonal matrix corresponding to the staggered magnetization. Similarly one can compute the staggered susceptibility χ defined as

$$\chi=\frac{1}{N}[\langle M^2\rangle-\langle M\rangle^2]. \tag{14}$$

This exact evaluation can, however, be done only for small systems since this procedure involves using very large matrices. For finite J, we have been able to do this calculation only for $L\leqslant 6$. For $J\to\infty$, the transfer matrices become block diagonal, and this means that one can perform separately the computations in each block that are of smaller size. In this case, we have been able to go up to system size $L=12$. Note that in this limit, we can also compute the thermodynamic properties in each sector. In Fig. 9, we have plotted the exact results for m obtained from the full partition function with $J=1$, as well as the results for m in the $p=2/3$ sector for infinite J. It is readily seen that our picture of the system getting stuck in the $p=2/3$ sector during the cooling run is correct.

The counter-intuitive results of the quenching process can also be understood using the above picture. After the quench, domains of spins pointing in and opposite to the direction of the staggered field begin forming. Only spins on the boundaries of the domains can flip, leading to motion of the domain walls. This motion is biased, favoring the growth of the domains aligned with the staggered field. Now we recall that any nonzero string configuration will have domains of misaligned spins spanning the entire lattice. Clearly, it is extremely unlikely that the biased domain growth process will lead to such configurations. We have checked in our simulations that as the system size is increased, the probability of the quench leading to the zero-string sector approaches unity. To further clarify this process, we show in Fig. 10 different stages in the evolution of a 24×24 system following a zero-temperature quench from a random initial state. The field is set at the value $h=0.05$. It can be seen that the domains of misaligned spins rapidly vanish. On the other hand, in Fig. 11 we show a $T=0.4$ equilibrium spin configuration and the result of quenching it to $T=0$. In this case the system gets stuck in the $p=2/3$ sector.

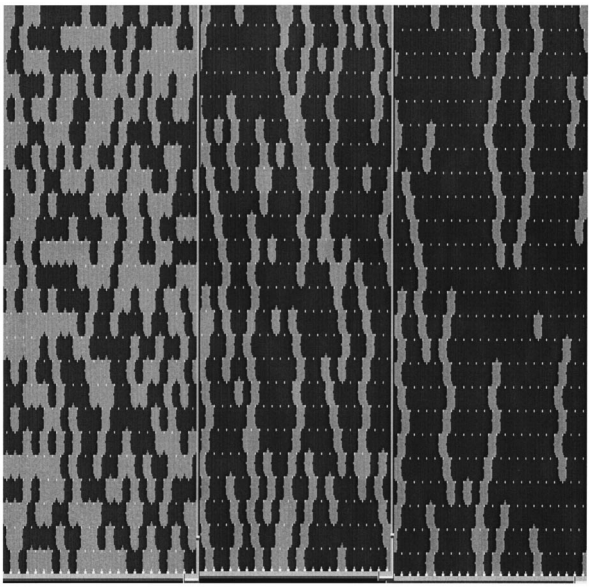

FIG. 10. Three stages in the evolution of the system, following a zero-temperature quench from a random initial state. The first is the initial configuration and the other two are configurations obtained after 2 and 4 MC sweeps. The dark and bright regions indicate spins pointing along and opposite to the direction of the staggered fields, respectively.

B. String dynamics

To speed up the dynamics, it is necessary to be able to efficiently change the number of strings. A straightforward way of doing this is to introduce moves that attempt to flip an entire vertical line of spins. Such moves are accepted or rejected according to the usual Metropolis rules. Combining these moves with the single-spin-flip ones makes the dynamics ergodic at zero-temperature in the absence of the field. In Fig. 12, we show the results of simulations with the string

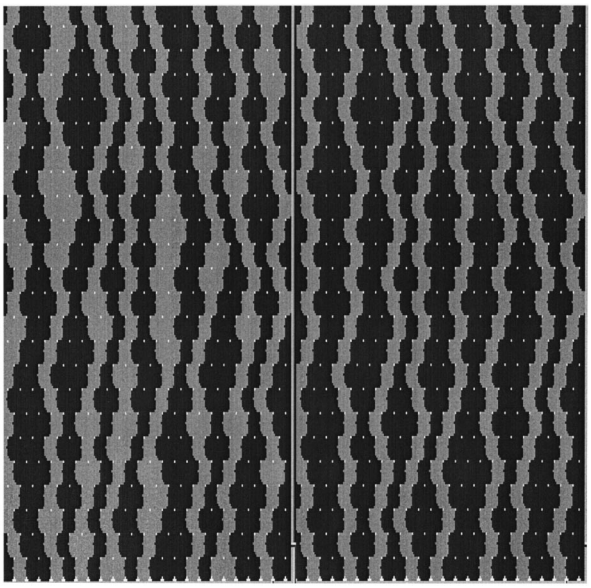

FIG. 11. A configuration that is at equilibrium at $T=0.4$ and the configuration resulting from quenching it to $T=0$. It can be seen that the final configuration consists of tightly bound strings and is the lowest-energy state in the $p=2/3$ sector.

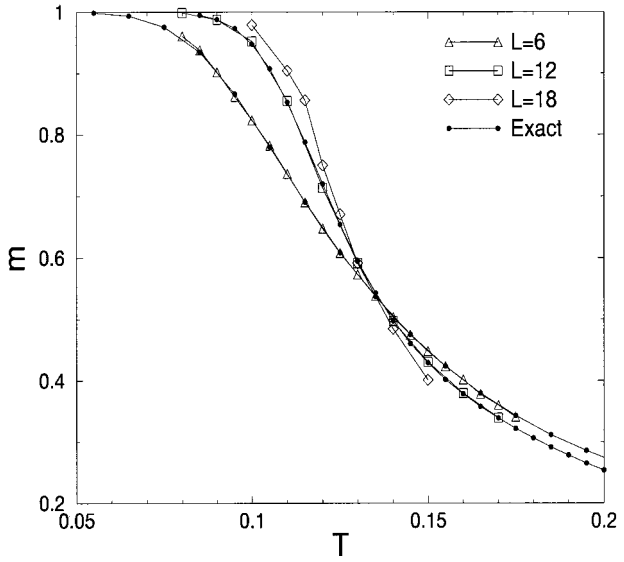

FIG. 12. Staggered magnetization m versus temperature T for $h=0.05$, $J=1$. The data for system sizes $L=6$, 12, and 18 were obtained from MC simulations using string dynamics. Exact transfer-matrix results for $L=6$ and for $L=12$ $(J\to\infty)$ are also shown.

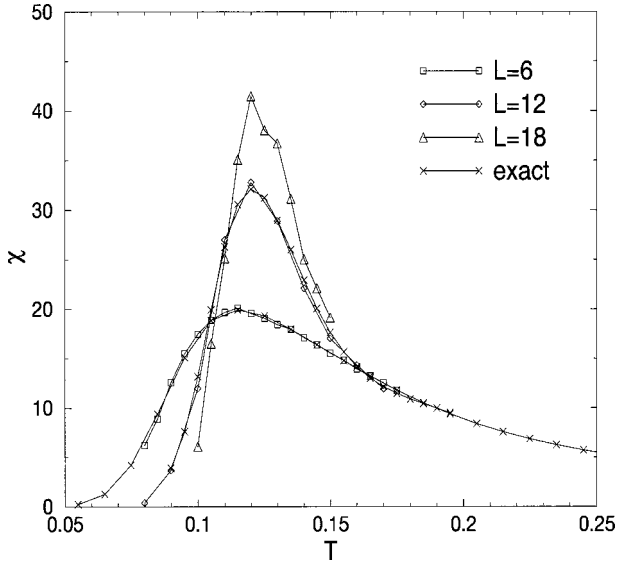

FIG. 13. Staggered susceptibility χ versus temperature T for $h=0.05$, $J=1$. The data for system sizes $L=6$, 12, and 18 were obtained from MC simulations using string dynamics. Exact transfer-matrix results for $L=6$ and for $L=12$ $(J\to\infty)$ are also shown.

dynamics, again for a 6×6 system. The values of J and h are the same as those for the data shown in Fig. 9, and the averaging is over the same number of MCS. The excellent agreement with the exact results shows that equilibration times have been greatly reduced. We have also shown in Fig. 12 simulation results for a 12×12 system. Again there is very good agreement with the exact results, which, as noted above, were obtained by setting $J\to\infty$.

To determine the existence of a phase transition, we have performed simulations with the above dynamics and studied the dependence of the staggered susceptibility χ on the system size for different values of the field. The results are summarized in Figs. 13, 14, and 15. The data in Fig. 13 correspond to a low-field value, $h=0.05$. The number of MCS used for computing the averages is 10^6, 10^7, and 4×10^8 for the three system sizes, $L=6$, 12, and 18, respectively. For system sizes $L=6$ and $L=12$, we also show the exact transfer-matrix results. Even though the $L=12$ transfer-matrix results are for $J\to\infty$, we find very good agreement with the simulation data. This is because excitations out of $\mathcal{G}$, which involve energies of order J, are very much suppressed at the low temperatures considered. The $L=18$ MC data are not as smooth as the data for smaller sample sizes, indicating that the errors in the calculation of averages are significant in spite of averaging over a very large number of MCS. Thus, even with the string dynamics, we have not been able to attain equilibration for systems with $L>18$.

The close agreement between the MC results for $J=1$ and the exact transfer-matrix results for $J\to\infty$ indicates that the MC results for the system sizes considered are representative of the $J\to\infty$ limit. In Sec. III, we established the existence of a finite-temperature phase transition in this limit. Our MC results indicate that this transition occurs near $T\simeq2.5h$, which is substantially higher than the lower bound, $h/\ln(2)$, derived in Sec. III. To determine whether this transition is a K-type, we have examined the dependence of χ_p, the peak value of the staggered susceptibility χ, on the system size L. In the $J\to\infty$ limit, the staggered susceptibility is proportional to the specific heat that diverges as $(T-T_c)^{-1/2}$ in a K-type transition. This implies that the susceptibility exponent $\gamma=1/2$, and the correlation length exponent ν is equal to 3/4. According to standard finite-size scaling,[11] χ_p then should be proportional to $L^{\gamma/\nu}=L^{2/3}$. As shown in Fig. 16, our numerical data are in good agreement with this expectation. We, therefore, conclude that our model undergoes a K-type transition in the $J\to\infty$ limit.

In Fig. 14, we show simulation results for an intermediate field value, $h=0.25$. In this case, for system sizes L

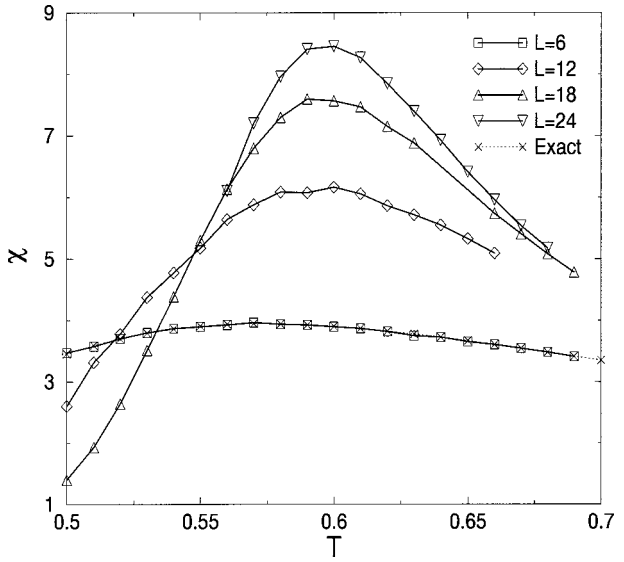

FIG. 14. Staggered susceptibility χ versus temperature T for $h=0.25$, $J=1$. The data for system sizes $L=6$, 12, 18, and 24 were obtained from MC simulations using string dynamics. Exact transfer-matrix results for $L=6$ are also shown.

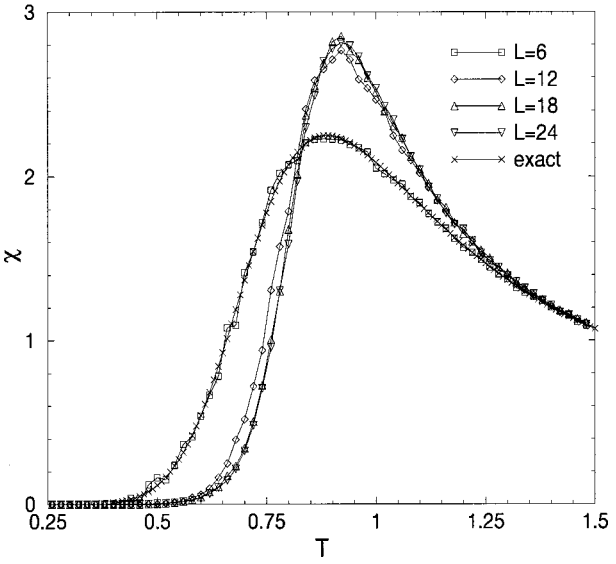

FIG. 15. Staggered susceptibility χ versus temperature T for $h=0.4$, $J=1$. The data for system sizes $L=6$, 12, 18, and 24 were obtained from MC simulations using string dynamics. Exact transfer-matrix results for $L=6$ are also shown.

$=6$, 12, 18, and 24, equilibrium values were obtained by averaging over 2×10^6, 5×10^6, 2×10^7, and 5×10^7 MCS, respectively. As in the $h=0.05$ case, the peak of χ occurs near $T\simeq2.5h$, and the peak value of χ increases as L is increased. Finally, in Fig. 15, we have shown the results for a high-field value, $h=0.4$. In this case, equilibration times are quite small and we can simulate relatively large systems without any difficulty. All the MC data shown in Fig. 15 were obtained with averaging over only 2×10^5 MCS. We find that in this case, the staggered susceptibility saturates for $L\geqslant12$, and clearly there is no phase transition.

In Fig. 16, we have plotted χ_p, the value of the staggered susceptibility at the peak, against the system size L for the

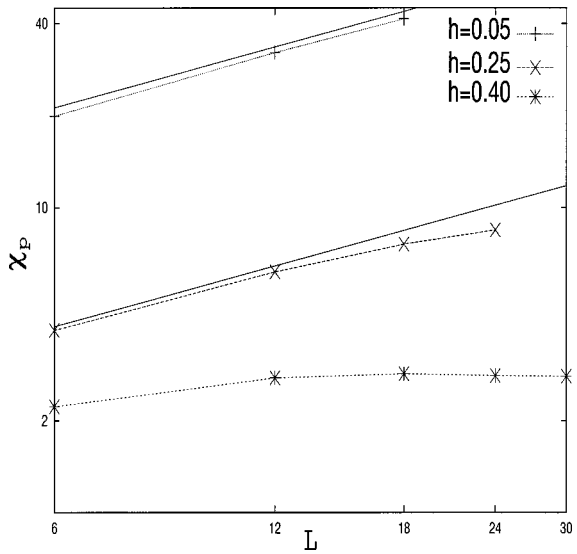

FIG. 16. The susceptibility maximum χ_p plotted against the system size L for three different values (0.05, 0.25, and 0.4) of the staggered field h. The solid lines correspond to the power-law form $\chi_p\propto L^{2/3}$.

three different fields. As noted above, we get $\chi_p\sim L^{2/3}$ for $h=0.05$. For $h=0.25$, the values of χ_p for $L=6$ and $L=12$ are consistent with this power-law form, but the data for higher values of L show deviations from this form and signs of saturation. Finally, for $h=0.4$, the peak value of χ clearly saturates for $L\geqslant12$.

Taken at face value, these results would imply that for $J=1$, there is a K-type transition for $h=0.05$, but no transition for $h=0.25$ and $h=0.4$. In other words, there is a phase transition for small h, which disappears beyond a critical value of the field. This naive interpretation of the data is questionable because a line of continuous phase transitions in the h-T plane is very unlikely to end abruptly at some point. A more plausible interpretation is that the system with finite J does not exhibit a true phase transition for any value of the staggered field—the signature of a phase transition found in the scaling behavior of the data for small h is a remnant of the transition in the $J\to\infty$ limit. The behavior of a system with finite J would differ from that in the $J\to\infty$ limit only if the values of the parameters J, T, and L are such that excitations out of the manifold $\mathcal{G}$ are not strongly suppressed. Since the typical value of the local field in a configuration in $\mathcal{G}$ is $2J$, the typical energy cost associated with a single-spin-flip excitation out of this manifold is $4J$. Since this excitation can occur at any site of the lattice, the free-energy cost of such an excitation is approximately given by $\delta F\simeq4J-2T\ln L$. Such excitations are likely to occur if $\delta F\leqslant0$, which corresponds to $L\geqslant L_c=e^{2J/T}$. The values of L_c at temperatures near the peak of χ are $\approx10^7$, 28, and 7.4 for $h=0.05$, 0.25, and 0.4, respectively. In view of the very large value of L_c for $h=0.05$, it is not surprising that the MC results for m and χ for $h=0.05$, $J=1.0$, and $L\leqslant18$ are essentially identical to the results for the same value of h in the $J\to\infty$ limit. The power-law scaling of the data for χ_p at $h=0.05$ can then be attributed to the occurrence of a phase transition in the $J\to\infty$ limit. The observation that for $h=0.25$, the numerical data for χ_p show deviations from power-law scaling with L and signs of saturation for $L\geqslant24$ is also consistent with this interpretation. The small value of L_c for $h=0.4$ implies that the effects of J being finite should be evident even in the small samples we consider. The fact that the data for $h=0.4$ clearly indicate the absence of any phase transition is, thus, consistent with the interpretation that there is no phase transition for finite J.

While the scenario described above is consistent with all our numerical data, we cannot be absolutely sure that it is correct—data for much larger systems would be needed for a conclusive answer to the question of whether a phase transition occurs for finite J. We note that even if our interpretation is correct, the behavior of finite samples with finite J would look very similar to that near a true phase transition if h/J is small. In such cases, the value of χ_p will continue to grow with L as a power law until L becomes comparable to L_c, at which point χ_p will saturate. Since L_c depends exponentially on J/h, it would be very large for $h/J\ll1$.

C. Cluster dynamics

We have also performed simulations using a cluster method. We briefly report our results here. This method was introduced by Kandel *et al.*[12] for the study of frustrated sys-

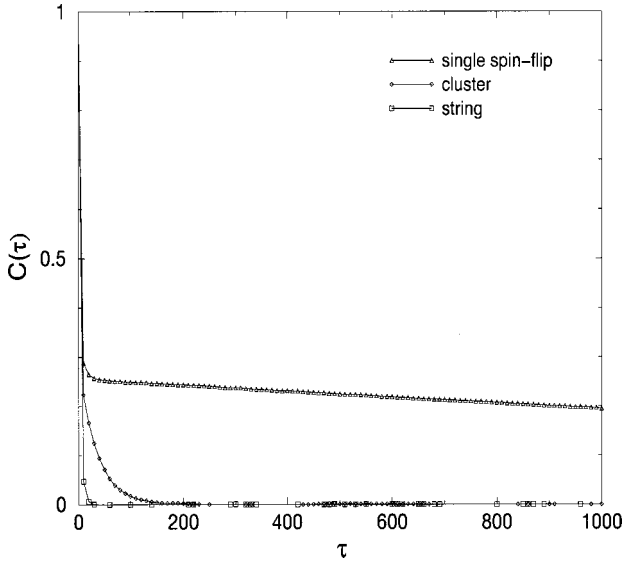

FIG. 17. Autocorrelation function $C(\tau)$ of the staggered magnetization, obtained from the three different dynamics at a comparatively high temperature, $T=0.4$. The data are for a 6×6 sample with $J=1$, $h=0.05$. The ''time'' τ is measured in units of MC steps per spin.

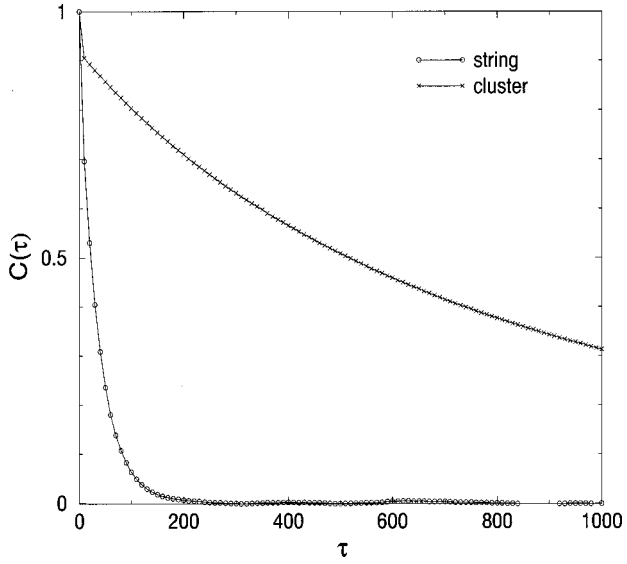

FIG. 18. Autocorrelation function $C(\tau)$ of the staggered magnetization, obtained from string and cluster dynamics at a low temperature, $T=0.125$. The data are for a 6×6 sample with $J=1$,$h=0.05$. The ''time'' τ is measured in units of MC steps per spin.

tems. Recently Zhang and Yang[13] have applied this algorithm to the zero-field TIAFM. We have modified this algorithm to take into account the presence of the staggered field. The cluster algorithm is usually implemented in two steps. In the first step, one performs a ''freeze-delete'' operation on the bonds using a fixed set of rules,[12,13] which results in the formation of independent clusters. The second step consists in flipping these clusters. In our modified algorithm, the first step is unchanged. The freeze-delete operations are exactly as in Ref. 13 and are effected without considering the energy associated with the staggered field. In the second step, we calculate the staggered-field energy of every cluster and then flip it using heat-bath rules. It can be proved that this procedure satisfies the detailed balance condition.

The cluster dynamics performs better than the single-spin-flip dynamics and we have been able to obtain equilibrium averages for a $L=6$ system ($J=1$, $h=0.05$) with 10^6 MCS. However, for bigger system sizes ($L\geqslant12$), we have not been able to achieve equilibration even with runs over 10^8 MCS. Thus this dynamics is much slower than the string dynamics. This is due to the following reason. While the cluster dynamics does allow the number of strings to change, the clusters formed at low temperatures are quite large and the probability of flipping them becomes very small. In order to obtain quantitative comparisons of the three different dynamics, we have studied the autocorrelation function,

$$C(\tau)=\frac{\langle M(\tau)M(0)\rangle-\langle M\rangle^2}{\langle M^2\rangle-\langle M\rangle^2}, \tag{15}$$

where M is the total staggered magnetization and τ is the ''time'' measured in units of MCS. In Figs. 17 and 18, we plot the results for $C(\tau)$ obtained from simulations using different dynamics at two different temperatures. The data correspond to a $L=6$ lattice and the averaging was carried out over 10^7 MCS in all the cases. We note that the single-spin-flip dynamics leads to a two-step relaxation—a fast one corresponding to equilibration within a sector and a slower one in which different sectors are sampled. The results shown in these figures also demonstrate the superiority of the string dynamics over the other two methods at both high and low temperatures.

V. SUMMARY AND DISCUSSION

In summary, we have studied the equilibrium properties of a triangular Ising antiferromagnet in the presence of an ordering field, which is conjugate to one of the degenerate ground states. We have addressed the question of whether a phase transition can occur in this system. Using a mapping of the TIAFM ground states to dimer coverings, we find that it is possible to obtain a very detailed description of the low-lying energy states. In the limiting case of the coupling constant $J\to\infty$, we show that the problem reduces to that of a set of nonintersecting strings with long-range interactions. For this limiting case, we prove existence of a transition that appears to be *K*-type. For finite *J*, we have studied the system using exact numerical evaluation of the staggered magnetization and susceptibility by transfer-matrix methods, and also by MC simulations using three different dynamics. We find that the dimer description also helps in understanding the dynamics and in finding methods of improving the efficiency of the MC simulation. A single-spin-flip dynamics is very inefficient in sampling different string sectors and at low temperatures, the system stays stuck within a sector and shows thermodynamic behavior corresponding to that sector. A cluster dynamics method improves over the single-spin-flip dynamics, but is still very slow at low temperatures. We have developed a dynamics that allows moves that add or remove pairs of strings. As expected, this greatly reduces equilibration times. However, even with this increased efficiency, we have not been able to equilibrate systems with $L>18$ in the interesting region of low-field values (h/J

$\ll 1$). Hence our results on possible phase transitions for finite J are inconclusive, although there are indications that a true phase transition does not occur for finite J.

We close with a few comments on possible connections of the system studied here with supercooled liquids near the structural glass transition. The phase transition we found in our model in the $J \to \infty$ limit is similar in nature to the Gibbs–Di Marzio scenario[14] for the structural glass transition. In the Gibbs–Di Marzio picture, the structural glass transition is supposed to be driven by an ''entropy crisis'' resulting from a vanishing of the configurational entropy as the transition is approached from the high-temperature side. A similar vanishing of the entropy occurs at the phase transition in our model. It is interesting to note in this context that a ''compressible'' TIAFM model in which the ground-state degeneracy is lifted by a coupling of the spins with lattice degrees of freedom has been proposed[16] as a simple spin model of glassy behavior. In view of these similarities with the structural glass problem, a detailed study of the dynamic behavior of our model would be very interesting.

ACKNOWLEDGMENTS

We thank Chinmay Das, Rahul Pandit, and B. Sriram Shastry for helpful discussions.

*Also at the Condensed Matter Theory Unit, Jawaharlal Nehru Center for Advanced Scientific Research, Bangalore 560064, India.

[1] G.H. Wannier, Phys. Rev. **79**, 357 (1950).
[2] J. Stephenson, J. Math. Phys. **5**, 1009 (1964).
[3] B. Nienhuis, H.J. Hilhorst, and H.W.J. Blöte, J. Phys. A **17**, 3559 (1984).
[4] R.M.F. Houtappel, Physica (Amsterdam) **16**, 425 (1950).
[5] W. Kinzel and M. Schick, Phys. Rev. B **23**, 3435 (1981).
[6] H.W.J. Blöte and H.J. Hilhorst, J. Phys. A **15**, L631 (1982).
[7] H.W.J. Blöte and M.P. Nightingale, Phys. Rev. B **47**, 15 046 (1993).
[8] S. Franz and G. Parisi, Phys. Rev. Lett. **79**, 2486 (1997); M. Cardenas, S. Franz, and G. Parisi, J. Phys. A **31**, L183 (1998).
[9] C.N. Yang and T.D. Lee, Phys. Rev. **87**, 410 (1952); M. Suzuki and M.E. Fisher, J. Math. Phys. **12**, 235 (1971).
[10] K. Binder and D. W. Herrman, *Monte Carlo Simulation in Statistical Physics* (Springer-Verlag, Berlin, 1988).
[11] *Finite Size Scaling*, edited by J. L. Cardy (Elsevier, Amsterdam, 1988).
[12] D. Kandel, R. Ben-Av, and E. Domany, Phys. Rev. B **45**, 4700 (1992).
[13] G.M. Zhang and C.Z. Yang, Phys. Rev. B **50**, 12 546 (1994).
[14] J.H. Gibbs and E.A. Di Marzio, J. Chem. Phys. **28**, 373 (1958); G. Adams and J.H. Gibbs, *ibid.* **43**, 139 (1965).
[15] An interacting string model related to the TIAFM has been studied by J.D. Noh and D. Kim, Phys. Rev. E **51**, 226 (1995).
[16] L. Gu and B. Chakraborty, in *Structure and Dynamics of Glasses and Glass Formers*, edited by C. A. Angell, K. L. Ngai, J. Kieffer, T. Egami, and G. U. Nienhaus, MRS Symposia Proceedings No. 455 (Materials Research Society, Pittsburgh, 1997).